Int J Cancer Manag. 2018 January; 11(1):e9402. doi: 10.5812/ijcm.9402.

Published online 2018 January 31. **Research Article**

Enhanced Anti-Cancer Capability of Ellagic Acid Using Solid Lipid Nanoparticles (SLNs)

Hamed Hajipour,[1] Hamed Hamishehkar,[2] Mohammad Rahmati-yamchi,[3] Dariush Shanehbandi,[4] Saeed Nazari Soltan Ahmad,[1] and Akbar Hasani[2,*]

[1]Student Research Committee and Department of Biochemistry and Clinical Laboratories, Faculty of Medical Sciences, Tabriz University of Medical Sciences, Tabriz, Iran
[2]Drug Applied Research Center, Tabriz University of Medical Sciences, Tabriz, Iran
[3]Biotechnology Research Center, Tabriz University of Medical Sciences, Tabriz, Iran
[4]Immunology Research Center, Tabriz University of Medical Sciences, Tabriz, Iran

[*]*Corresponding author*: Akbar Hasani, Department of Biochemistry and Clinical Laboratories, Faculty of Medical Sciences, Tabriz University of Medical Sciences, Tabriz, Iran. Tel: +98-9141076650, Fax: +98-4133364667, E-mail: bioakbarhasani@gmail.com

Received 2016 October 18; **Revised** 2017 February 20; **Accepted** 2018 January 24.

Abstract

Background: Ellagic acid (EA) is a polyphenol, whose anti-cancer properties have been demonstrated in several cancer studies, but the poor water solubility and low bioavailability have limited its therapeutic potential.
Objectives: The present study proposed to develop solid lipid nanoparticles (SLNs) as a delivery system for improving the anti-cancer capability of EA on prostate cancer cell line.
Methods: EA-loaded SLNs were prepared by hot homogenization technique and characterized by different techniques. Cytotoxicity of EA and EA-loaded SLNs on prostate cancer cell line (PC3) was evaluated by 3-(4, 5-Dimethylthiazol-2-yl)-2, 5-diphenyltetrazolium bromide (MTT) assay, and nucleus condensation, or chromatin fragmentation (the signs of apoptosis) were studied by 4'-6-diamidino-2-phenylindole (DAPI) staining. The expression of B-cell lymphoma 2 (Bcl-2) and Bcl-2-associated X protein (Bax), which are involved in apoptosis, were evaluated by quantitative reverse transcription polymerase chain reaction (qRT-PCR).
Results: The nanoparticles with appropriate characteristics (particle size of 96 nm and Encapsulation Efficiency of 88%) were prepared. The in vitro drug release profile showed a burst release in the first hours and followed by a sustained EA release until 72 hours. EA-loaded SLNs displayed a good stability for 4 weeks of storage at 4 - 8°C. Cytotoxicity evaluations demonstrated that EA-loaded SLNs prevented prostate cancer cells growth in a low IC50 value compared to the EA. The results of qRT-PCR demonstrated that EA causes up-regulation of Bax and this regulation intensified when EA was loaded into SLNs, but there was no punctual correlation between the EA and EA-loaded SLNs in down-regulation of Bcl-2.
Conclusions: The results strengthen our hope that loading EA into SLNs could possibly overcome the therapeutic limitations of EA and make it more effective in prostate cancer therapy.

Keywords: Ellagic Acid, Prostate Cancer, Solid Lipid Nanoparticles, Cancer, Solid Lipid Nanoparticles; Cancer; SLN

1. Background

Prostate cancer is the second most commonly recognized cancer and the sixth leading cause of cancer death in males (1). About 80% of men above 80 years old suffer from prostate cancer; so, it is a considerable health and economic burden in our current aging population (2). Ellagic Acid (EA) (C14H6O8) is a polyphenol found in berries, walnuts and pomegranates, and exhibits wide spectrum health beneficial properties (3), especially anti-cancer characteristics such as anti-proliferative (4) and anti-angiogenic activities (5). EA was reported to inhibit cell proliferation and cell cycle progression of bladder (6), colorectal (7), and breast cancer (8). In spite of EAs benefits, the poor water solubility (9.7 μg/mL at pH 7.4) and extensive first pass intestinal and hepatic metabolisms and, consequently, low oral bioavailability of EA have limited the therapeutic potential of the molecule to mature into clinical trials (9, 10). In order to improve its therapeutic value, it is proposed to employ a nanoparticulate delivery system. The enhanced drug bioavailability of nanoparticles is corresponded to the fact that particles in the nano-size range are efficient in crossing permeability barriers (11). It has been indicated that nanoparticles enter the systemic circulation through lymphatic transport, which enhances oral drug absorption. Moreover, bypassing the liver through lymphatic transport leads to a reduced first-pass metabolism and, consequently, enhances oral drug bioavailability (12). Among drug carriers, SLNs have at-

tracted increasing attention as a potential drug delivery carrier due to their physical stability, protection of labile drugs from degradation, low toxicity, and ability to immobilize both hydrophilic and hydrophobic drugs in the solid matrix (13). Solid lipid nanoparticles are colloidal carrier system composed of a high melting point lipids as a solid core coated by surfactants that offer an attractive means of drug delivery, particularly for improving bioavailability of poorly water soluble molecules (14, 15). Their small size allows nanocarriers to overcome non-selective uptake by the reticuloendothelial system and achieve passive targeting through enhanced permeability and retention (EPR) in tumor therapy (16).

2. Objectives

The aim of the present study was to prepare and optimize EA-loaded SLNs and explore the enhanced anti-tumor activity against PC3 human prostate cancer cell line. The probable signaling pathway of EA-loaded SLNs in cancer prevention and impact on gene expression of Bcl-2 (B-cell lymphoma 2) and Bax (Bcl-2-associated X protein) were investigated and compared with EA.

3. Methods

3.1. Material

EA, 3- (4,5- Dimethylthiazol- 2- yl)-2, 5- diphenyltetrazolium bromide (MTT), Poloxamer 407, RPMI 1640, fetal bovine serum (FBS), and Penicillin-Streptomycin were purchased from sigma aldrich company. Precirol® ATO 5 was supplied from Gattefosse (France). PC3 prostate cancer cell line was obtained from national cell bank of Iran (Pasteur institute, Iran). RNX-Plus solution for total RNA isolation and RevertAid first strand cDNA Synthesis Kit were purchased from Sinaclon company (Iran) and thermo scientific (thermo scientific, Schwerte, Germany), respectively. SYBR Premix Ex Taq II was prepared from Takara Company. (Japan).

3.2. Preparation and Characterization of EA-Loaded SLNs

EA-loaded SLNs were prepared by hot homogenization method. Briefly, the lipid phase, consisting of different concentrations of Precirol and Tween-80 as a surfactant was heated up to 70°C to be melt. EA was dissolved in dimethyl sulfoxide (DMSO) and injected into the molten lipid phase. Subsequently, the aqueous phase containing Poloxamer 407 in water at the same temperature was added into the lipid phase dropwise under high speed homogenizer (Heidolph, Germany) with stirring rate of 21000 rpm. After homogenization, the produced nanoemulsion was recrystallized to SLNs by cooling down to room temperature. Twelve formulations were fabricated based on changes in lipid, surfactants, and external aqueous phase volume (Table 1). The size, polydispersity index (PDI), and zeta potential values of the EA-loaded SLNs were measured by dynamic light scattering technique (Nano ZS, Malvern Instruments, The UK). The size of the particles was reported by intensity and expressed by the Z-Average value. In order to investigate the morphological behaviors of nanoparticles, SLNs were observed with Scanning Electron Microscopy (SEM) (KYKY-EM3200, KYKY Technology Development Ltd., China).

3.3. Drug Encapsulation Efficiency (EE) and Loading Capacity (LC)

The EE (%) and LC values of EA-loaded SLNs were determined by filtration method, using centrifugal filter tube (Amicon® Ultra-15 with molecular weight cutoff of 100 kDa, Millipore, USA). To accurately calculate the EE, unloaded EA first should be dissolved and, then, separated from the dispersed SLNs. Therefore, a sample was taken from the preparation (containing SLNs and probable unloaded EA), diluted with ethanol to dissolve the EA particles (ethanol does not dissolve the Precirol®), and finally passed through Amicon filters by centrifugation at 5000 rpm for 10 minutes to separate the dissolved EA from the SLNs. The clear solution in the bottom of Amicon tube was used for EA determination by ultraviolet-visible spectrophotometer (Ultrascope 2000®, pharmacia biotech, UK) at λ_{max} 256 nm. The EE and LC values of EA-loaded SLNs were calculated, using the following formulas:

$$EE\,(\%) = \frac{C_t - C_{aq}}{C_t} \times 100 \quad (1)$$

$$LC\left(\frac{mg}{g}\right) = \frac{W_{dl}}{W_{np}} \quad (2)$$

where, C_t was the total added drug concentration, C_{aq} was the unloaded drug concentration, W_{dl} was the weight of drug loaded into SLNs, and W_{np} was weight of used solid lipid for the fabrication of SLNs.

3.4. In Vitro Release Study

Drug release studies were performed in simulated physiological (Phosphate-buffered saline (PBS) pH 7.4, 37°C) and cancerous tissue (PBS pH 6.5, 40°C) conditions. DMSO (1 mL) was added to PBS (19 mL) to provide sink condition for in vitro EA release from the SLNs. In each drug-release experiment, 1 mL of prepared SLNs was transferred into a cellulose acetate dialysis bag and was inserted in

Table 1. Composition and Characteristics of Prepared EA-Loaded SLNs[a]

Formulation Code	Precirol (g)	Tween (mg)	Poloxamer (mg)	Aqueous Phase (mL)	Size (nm)	PDI	EE (%)	LC (mg/g)
F1	0.8	-	800	40	490.4 ± 2.9	0.53 ± 0.01	95.2 ± 1.8	9.52 ± 0.17
F2	1	-	1000	40	779.2 ± 6.1	0.65 ± 0.02	97.2 ± 1.3	7.78 ± 0.10
F3	0.6	-	600	40	330.0 ± 5.5	0.59 ± 0.01	90.4 ± 1.9	12.05 ± 0.26
F4	0.6	5	600	40	279.1 ± 3.5	0.59 ± 0.01	94.7 ± 2.1	12.63 ± 0.28
F5	0.6	10	600	40	321.4 ± 4.4	0.54 ± 0.02	96.5 ± 1.5	12.87 ± 0.20
F6	0.6	5	300	40	205.6 ± 3.7	0.50 ± 0.02	95.5 ± 1.9	12.73 ± 0.26
F7	0.5	5	300	40	172.3 ± 2.1	0.56 ± 0.01	94.2 ± 2.2	15.07 ± 0.35
F8	0.25	-	150	20	136.3 ± 2.5	0.54 ± 0.01	85.3 ± 1.7	27.32 ± 0.56
F9	0.25	5	150	20	141.0 ± 2.4	0.51 ± 0.01	92.2 ± 2.1	29.51 ± 0.69
F10	0.2	5	120	20	96.2 ± 2.5	0.28 ± 0.01	88.8 ± 2.4	35.56 ± 0.97
F11	0.2	5	200	20	207.6 ± 2.3	0.34 ± 0.01	91.1 ± 1.5	36.43 ± 0.61
F12	0.2	5	150	20	111.1 ± 3.0	0.25 ± 0.01	94.1 ± 0.9	37.73 ± 0.46

Abbreviation: EE, encapsulation efficiency; LC, loading capacity; PDI, polydispersity index.
[a] Data is expressed as ± SD (n=3).

a glass holder that contained 20 mL of release medium. The release medium was withdrawn at predetermined time intervals and it was analyzed, using an ultraviolet-visible spectrophotometer at λ_{max} 256 nm to determine the amount of EA released. The release rate of EA was calculated from the following formulas:

$$\text{Released rate} = \frac{ReleasedEA}{TotalEA} \times 100 \quad (3)$$

3.5. Cell Culture and Cell Viability Assay

Human prostate cancer cell line (PC3) was grown in RPMI-1640 supplemented with 10% FBS, 1% penicillin streptomycin, and 2 g/L sodium bicarbonate at 37°C in humidified atmosphere. Cytotoxicity of EA-loaded SLNs and EA were determined by MTT assay. In brief 10^4 cells/well were seeded in a 96 well plate and were treated with the different concentrations of EA (dissolved in 0.5 % DMSO) and equivalent doses of EA-loaded SLNs and blank SLNs for 24, 48, and 72 hours. After appropriate time, medium of all wells were removed, 50 μL of 5 mg/mL MTT was dissolved in PBS, and150 μL of fresh medium was added to each wells and incubated for 4 hours at 37°C. Then, formazan crystals were dissolved in DMSO. Absorbance was measured at 570 nm, using a spectrophotometric plate reader (ELx 800, Biotek, CA).

3.6. DAPI Staining Assay

In order to determine nucleus condensation or chromatin fragmentation (the signs of apoptosis), 4'-6-diamidino-2-phenylindole (DAPI) staining was carried out. In brief, 3×10^5 PC3 cells/well were harvested in the six-well plates containing 12 mm cover-slips and, consequently, treated with EA, EA-loaded SLNs, and DMSO as a control. Then, cells were fixed with 4% paraformaldehyde and permeabilized in 0.1% (w/v) Triton X-100, washed with PBS, and stained with DAPI. Cells were evaluated under a fluorescence microscope (Olympus microscope Bh2-RFCA, Japan).

3.7. Cell Uptake Study

Rhodamin B was used as a fluorescence probe to investigate the cellular uptake of Rhodamin-loaded SLNs. Unencapsulated Rhodamin B was removed by filtration, using centrifugal filter devices. In brief, 3×10^5 cells/well were harvested in six-well plates containing 12 mm cover-slips and incubated until their adherence on cover-slips. Then, adherent cells were treated with Rhodamin-loaded SLNs, diluted in medium, during an incubation period of 4 hours. The cells were washed 5 times with PBS and imaged with a fluorescence microscope. All the experimental steps were performed considering light protection with aluminium sheet to avoid fluorescent dequenching.

3.8. RNA Extraction, Reverse Transcription and Analysis of Gene Expression

The cells were treated with IC50 concentrations of EA and equivalent doses of EA-loaded SLNs for 48 hours. Then, for extraction of RNA, RNX-plus solution (Sinaclon, Iran) was used according to the manufacturer's protocol. Then, the quality and quantity of isolated RNA were

assessed by nanoDrop (ND-1000, NanoDrop technology, Australia). The RNA was, then, transcribed to complementary DNA (cDNA), using a reverse transcriptase kit (thermo scientific, Schwerte, Germany) according to the instruction manual. Quantitative reverse transcription polymerase chain reaction (qRT-PCR) method was performed based on the SYBR Green chemistry to analyze the expression levels of Bax and Bcl-2 relative to the B-actin as a housekeeping gene. The following primers were used for the amplification of human Bax, Bcl-2, and B-actin: Bax (forward) 5'- TTGCTTCAGGGTTTCATCCA -3' and (reverse) 5'- GACACTCGCTCAGCTTCTTG -3'; Bcl-2 (forward) 5'-GTCATGTGTGTGGAGAGCG-3' and (reverse) 5'-ACAGTTCCACAAAGGCATCC-3'; and B-actin (forward) 5'-TCCCTGGAGAAGAGCTACG-3' and (reverse) 5'-GTAGTTTCGTGGATGCCACA-3'. In brief, about 1 μL (10 PM/μL) of each specific primers and 1 μL of each cDNA sample were added to PCR tubes containing SYBR-Green Master Mix (7.5 μL), and sterile water (5.5 μL). The sample tubes were placed into the real time rotary analyzer (Rotor-Gene 6000, Corbet Life Science, Australia) with the following settings: 45 cycles of 4-step PCR (95°C - 5 minutes, 95°C - 15 seconds, 59°C - 35 seconds, 72°C - 15 seconds) for both Bax and B-actin and 45 cycles of 4-step PCR (95°C - 10 minutes, 95°C-15 seconds, 63°C - 35seconds, 72°C - 15seconds) for Bcl-2. The fold changes in gene expression were calculated by $2^{-\Delta\Delta Ct}$ method.

3.9. Statistical Analyses

All results were presented as the means $\pm$ standard deviation (SD) calculated by Microsoft® Excel 2013. The mean values were compared, using Student's t test to compare the mean differences between 2 groups. P Value less than 0.05 was considered significant.

4. Results

4.1. Preparation and Characterization of EA-Loaded SLNs

The characteristics of twelve formulations are shown in Table 1. Regarding the higher LC, nanoscale particle size and narrow polydispersity, the best formulation was composed of 200 mg Precirol, 120 mg Poloxamer, and 5 mg Tween-80 as surfactants and stabilizer of particulate system (F10). The polydispersity index (PDI) of F10 (about 0.28) suggests a relatively narrow size distribution. Generally, PDI $<$ 0.5 confirms the monodispersity of nanosized particles (17). Dynamic light scattering (DLS) graph of optimized formulation (F10) was presented in Figure 1A. The optimized formulation (F10) was selected for the rest experiments. The SEM image (Figure 1B) approved that nanoparticles had a near spherical shape and their size were around 100 nm, confirming the results obtained from DLS. Spherical subject had the minimum surface area to volume ratio that might minimize the surface tension between the lipids and the aqueous phase, thus, leading to thermodynamic stability (18). Although the observed zeta potential value (-19.9 mV) (Figure 1C) might help the stability of SLNs by electrostatic repulsion effect, the effective zeta potential value was considered to be less than -30 mV and greater than +30 mV (19).

4.2. EA Release from SLNs

Release behavior of the nanoparticles was studied during 72 hours. The results demonstrated a strong initial burst release of EA in the first several hours followed by a subsequent prolonged release. The results also revealed that the percentage of cumulative release of EA were enhancing with increase in temperature and decrease in pH (Figure 1D).

4.3. Cytotoxic Effects of EA and EA-Loaded SLNs

The cytotoxicity of EA and EA-loaded SLNs were examined for their anti-proliferative activity in human prostate cancer based on MTT assay. The data analysis of the cytotoxicity assay showed that IC50s of EA and EA-loaded SLNs on PC3 cell line were 82 and 61 μM for 48 hours and 65 and 51 μM for 72 hours, respectively (Figure 2). The result showed that intact EA and EA-loaded SLNs decreased the growth of PC3 cells in a dose and time dependently manner. As revealed in graph, in 48 hours and 72 hours, the greater degree of anti-proliferation was detected for almost all doses of EA-loaded SLNs, when compared to EA. The results showed that blank SLNs exhibited no significant toxicity up to 50 μM of equivalent doses of EA. That is why SLNs are introduced as a biocompatible drug delivery carrier (20).

4.4. DAPI Staining

Nucleus morphology is a simple factor for determination of healthy, apoptotic, and necrotic cells. We investigated the inductions of apoptosis by DAPI staining, using fluorescent microscopy (Figure 3). The images of DAPI stained cells showed that EA loaded SLNs (Figure 3D) induce nucleus condensation or chromatin degradation more considerably than EA (Figure 3C) at the equal concentration and time treatment. Untreated cells (Figure 3A) and cells treated with DMSO 5% (Figure 3B) were used as negative and positive controls, respectively.

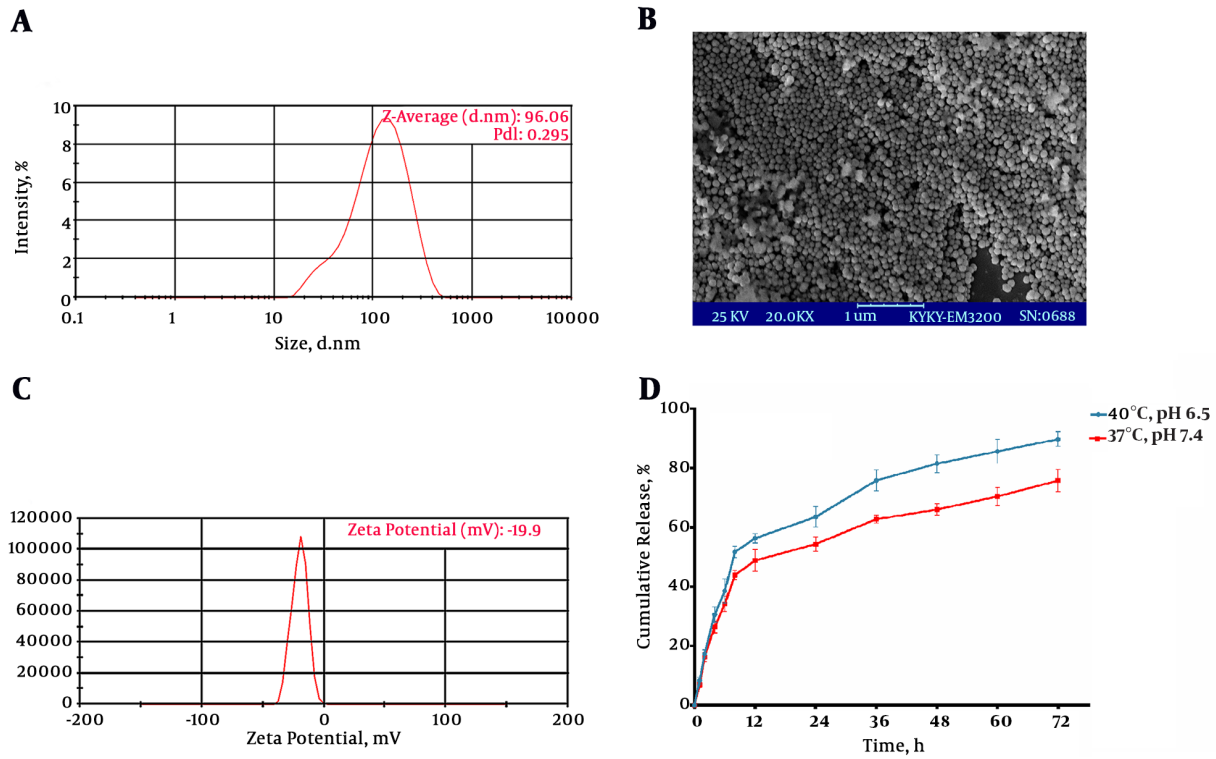

Figure 1. A, Size and polydispersity index (PDI) of optimized formulation based on Table 1 (F10); **B**, Scanning electron microscopy (SEM) image of F10; **C**, Zeta potential distribution of F10; **D**, Cumulative release of Ellagic acid (EA) from SLNs under a physiological (pH 7.4, 37°C) and cancerous tissue (PBS pH 6.5, 40°C) conditions.

4.5. Uptake of SLNs in Cells

In order to approve the uptake of SLNs, cells were incubated 4 hiurs with Rhodamin-loaded SLNs and were analyzed by fluorescence microscopy. As a negative control, cells were incubated with blank SLNs, separately under the same experimental conditions. Cells cultured with blank SLNs showed no fluorescence inside the cells, while an intense red fluorescence was observed inside the cells cultured with Rhodamin-loaded SLNs, conforming to a large number of Rhodamin-loaded SLNs that were internalized to cells (Figure 3E).

4.6. Quantitative Real-Time PCR

In order to understand the molecular mechanism, by which EA induced apoptosis, we analyzed the expression levels of Bax and Bcl-2 after the treatment of PC3 cells with EA and EA-loaded SLNs, using qRT-PCR. The level of Bax and Bcl-2 mRNA were normalized to mRNA level of the uniformly expressed housekeeping gene, B-actin, within each sample (Figure 4). The data showed that the treatment of PC3 cells with 61 μM EA, 61 μM EA-loaded SLNs, 82 μM EA, and 82 μM EA-loaded SLNs caused 1.47, 2.01, 1.89, and 2.39 fold increases in the expression level of Bax mRNA, respectively. The qRT-PCR data demonstrated that treatment of PC3 cells with EA and EA-loaded SLNs causes up-regulation of Bax mRNA level in dose-dependent manner and EA loaded in SLN is more effective than EA in this regulation. Although there was a considerable decrease in the expression of Bcl-2 mRNA levels in all of the treated samples with EA and EA-loaded SLNs compared to control, the changes were not statistically significant ($P > 0.05$).

5. Discussion

Based on the results, loading EA into SLNs could enhance the anti-cancer capability of EA against PC3 prostate cancer cells. Recent studies have shown that EA have potential biological activity. Nevertheless, its low bioavailability and low average individual consumption (around 343 mg EA per year) are great challenges for its beneficial functions (21). The nanocarriers can increase the bioavailability of poorly bioavailable drugs due to their specialized uptake mechanism (22). The physicochemical characteristics of SLNs such as size and drug loading efficiency are

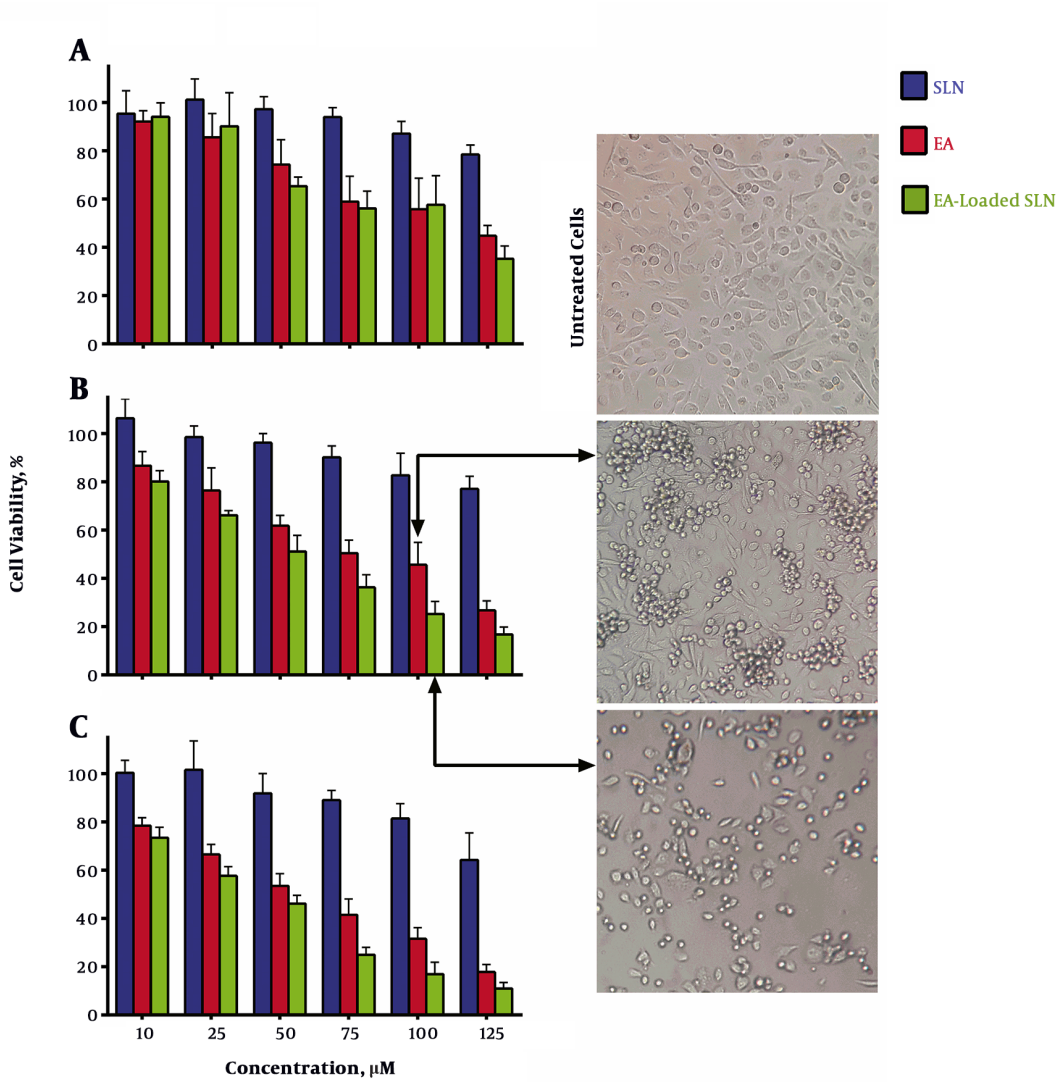

Figure 2. Cytotoxic effects of Ellagic acid (EA) vs. EA-loaded SLNs in **(A)** 24 hours, **(B)** 48 hours, and **(C)** 72 hours on PC3 cells. The figure illustrates that EA-loaded SLNs are more anti-proliferative when compared with EA in 48 and 72 hours, but there are no significant difference between 2 groups in 24 hours ($P > 0.05$). Data are presented as mean ± standard deviation (n = 3).

dependent on preparation process and the composition of SLNs (23). In this study, the characteristics of optimum formulation approve the appropriateness of the preparation process. The data of this study showed that Tween-80 as oil phase surfactant could increase the EA encapsulation. The size of nanoparticles used in a drug delivery system should be large enough (> 30 nm) to prevent their elimination by renal excretion, but small enough (up to 200 nm) to escape rapidly taken up by the mononuclear phagocyte system cells (24). Kind and concentration of emulsifier have significant effect in particle size. The higher concentrations of the emulsifier reduced the surface tension and facilitated particles dispersion during homogenization (25). The results of the present study showed that emulsifier (poloxamer) up to 75% of lipid supports the stability of nanoparticles, but when poloxamer is higher than this amount, it increases the size of nanoparticles. Zeta potential is another important factor for predicting the stability of nanoparticles. The high zeta potential value implies high electric surface charge on nanoparticles, which can lead to strong repulsive forces among nanoparticles to prevent it from aggregation (26). In contrast, the low

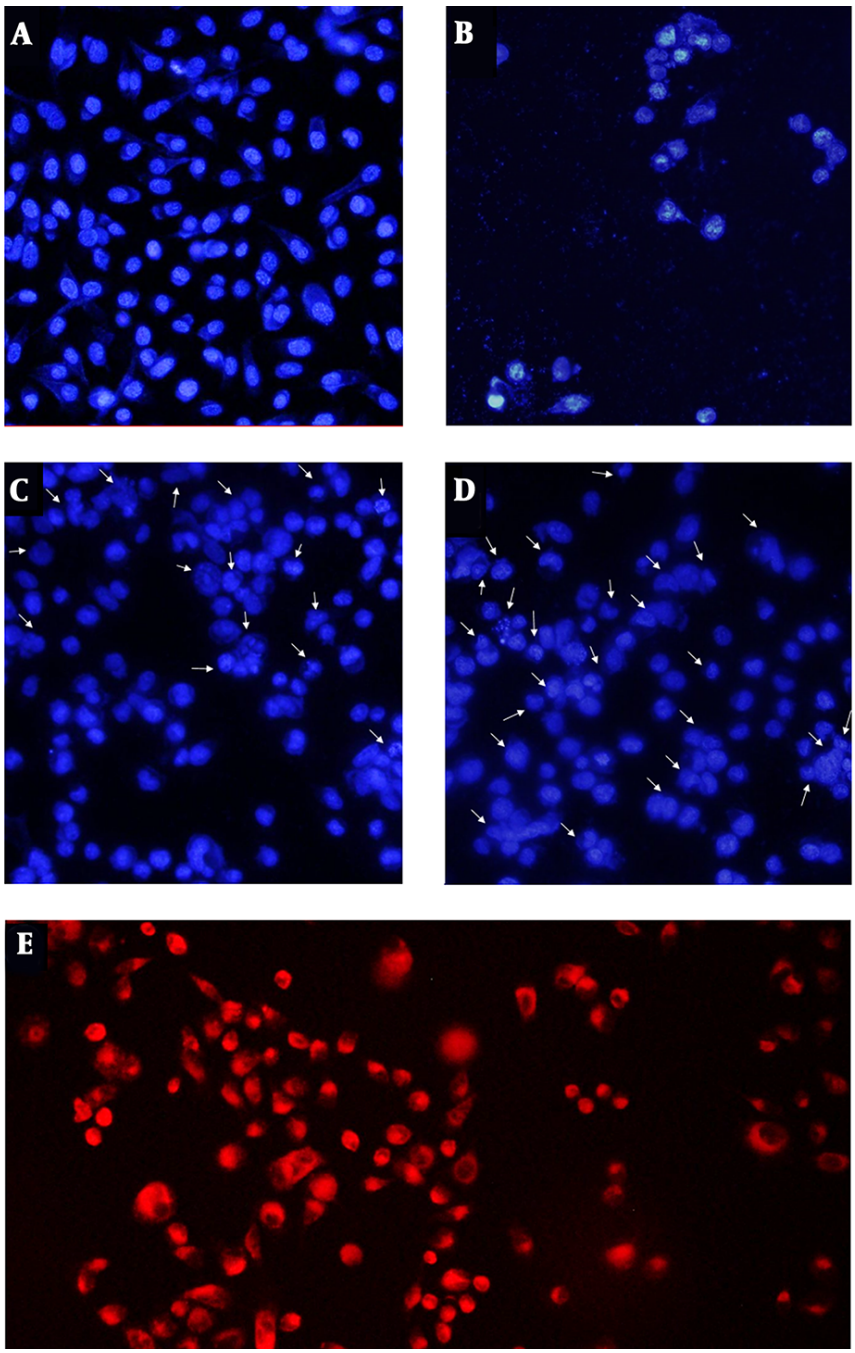

Figure 3. Fluorescent images of DAPI stained PC3 cells following a 48 hour exposure by **(A)** untreated, **(B)** DMSO 5%, **(C)** 61 μM EA and, **(D)** 61 μM EA-loaded SLNs. **(E)** Fluorescence microscope images of Rhodamine B-loaded SLNs uptake. (The arrows show nuclear condensation)

value of the zeta potential is indicated to display better permeability across cell membranes (27). The zeta potential of selected formulation supports reasonable stability, either even it is not too high to afraid from cell membrane. The study of drug release showed fast release in the initial hours, referring to the presence of drugs on or near the surface of nanoparticles, and subsequent sustained release could be caused by the diffusion of drugs inside the

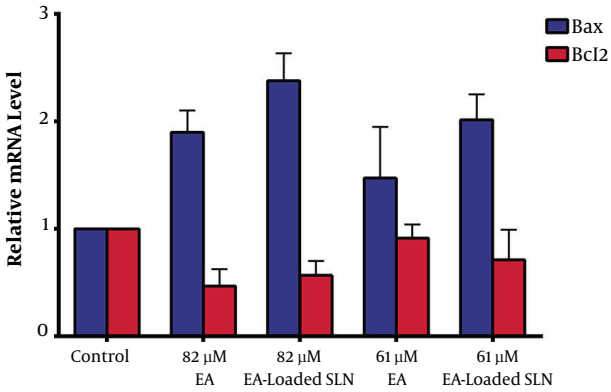

Figure 4. Effects of EA and EA-loaded SLNs on Bax and Bcl-2 mRNA expression levels in PC3 cells after 48 hours. EA up-regulate the Bax expression and it is more effective when loaded in SLNs. This chart shows down-regulation of Bcl2 when treated by EA, but it is not significant ($P > 0.05$)

nanoparticles (28). The results of this study verified that SLNs could be a hopeful drug delivery system for the sustained release of hydrophobic drugs in cancer treatments. This claim is supported by our cytotoxicity results, which showed that EA loaded SLNs were more effective than EA on PC3 cell line. In line with this investigation, Arulmozhi et al. showed EA encapsulated into chitosan nanoparticles has significant cytotoxicity against human oral cancer cell line (KB) in a dose-dependent manner with a very low IC50 value compared to the EA (26). Recently, NF-kB, cyclin D1, p21cip1/waf1, and p53 have been introduced as molecular targets, whereby EA caused apoptosis (29). Furthermore, Malik et al. have shown that EA administered the treatment of prostate cancer that decreases the Bcl-2 protein level and increases the Bax protein level (30). But, Bcl-2 and Bax mRNA expression have not been investigated. In the present study, an apparent increase in Bax mRNA expression levels was observed when the PC3 cells were treated with EA and EA-loaded SLNs (Figure 4). The up-regulation of Bax mRNA level intensified after cell treatment with EA-loaded SLNs. Bcl-2 and Bax are 2 members of the Bcl-2 family, which play converse roles in apoptosis (31). Bax promote cytochrome c release from the mitochondria, which eventually leads to apoptosis, but Bcl-2 promotes cell survival by inhibiting factors, which activate caspases (32). The results of this study suggest that loading EA in SLNs make it more effective than EA in up-regulation of Bax and this regulation can be one of the molecular mechanisms, through which EA induces apoptosis in PC3 cells.

In conclusion, loading EA into SLNs makes it more capable in the prevention of prostate cancer cell growth. More studies are needed to evaluate the anti-cancer effect of EA-loaded SLN on animal model, but the results strengthen our hope that loading EA into SLNs could possibly overcome the therapeutic limitations of EA and make it more effective in prostate cancer therapy.

Acknowledgments

This is a report of a database from thesis registered in faculty of medicine, Tabriz University of Medical Sciences (thesis No. 92/2-8/15) and financially supported by drug applied research center of the same university (grant No. 92/1113).

Footnotes

Authors' Contribution: None declared.

Conflict of Interest: None declared.

Financial Disclosure: None declared.

References

1. Jemal A, Bray F, Center MM, Ferlay J, Ward E, Forman D. Global cancer statistics. *CA Cancer J Clin*. 2011;**61**(2):69–90. doi: 10.3322/caac.20107. [PubMed: 21296855].
2. Chiam K, Ricciardelli C, Bianco-Miotto T. Epigenetic biomarkers in prostate cancer: Current and future uses. *Cancer Lett*. 2014;**342**(2):248–56. doi: 10.1016/j.canlet.2012.02.011. [PubMed: 22391123].
3. Häkkinen SH, Kärenlampi SO, Mykkänen HM, Heinonen IM, Törrönen AR. Ellagic acid content in berries: Influence of domestic processing and storage. *Europ Food Res Technol*. 2000;**212**(1):75–80. doi: 10.1007/s002170000184.
4. Vanella L, Barbagallo I, Acquaviva R, Di Giacomo C, Cardile V, Abraham NG, et al. Ellagic acid: cytodifferentiating and antiproliferative effects in human prostatic cancer cell lines. *Curr Pharm Des*. 2013;**19**(15):2728–36. [PubMed: 23092326].
5. Vanella L, Di Giacomo C, Acquaviva R, Barbagallo I, Li Volti G, Cardile V, et al. Effects of ellagic Acid on angiogenic factors in prostate cancer cells. *Cancers (Basel)*. 2013;**5**(2):726–38. doi: 10.3390/cancers5020726. [PubMed: 24216999].
6. Li TM, Chen GW, Su CC, Lin JG, Yeh CC, Cheng KC, et al. Ellagic acid induced p53/p21 expression, G1 arrest and apoptosis in human bladder cancer T24 cells. *Anticancer Res*. 2005;**25**(2A):971–9. [PubMed: 15868936].
7. Larrosa M, Tomas-Barberan FA, Espin JC. The dietary hydrolysable tannin punicalagin releases ellagic acid that induces apoptosis in human colon adenocarcinoma Caco-2 cells by using the mitochondrial pathway. *J Nutr Biochem*. 2006;**17**(9):611–25. doi: 10.1016/j.jnutbio.2005.09.004. [PubMed: 16426830].
8. Losso JN, Bansode RR, Trappey A2, Bawadi HA, Truax R. In vitro antiproliferative activities of ellagic acid. *J Nutr Biochem*. 2004;**15**(11):672–8. doi: 10.1016/j.jnutbio.2004.06.004. [PubMed: 15590271].
9. Bala I, Bhardwaj V, Hariharan S, Kumar MN. Analytical methods for assay of ellagic acid and its solubility studies. *J Pharm Biomed Anal*. 2006;**40**(1):206–10. doi: 10.1016/j.jpba.2005.07.006. [PubMed: 16111850].
10. Murugan V, Mukherjee K, Maiti K, Mukherjee PK. Enhanced oral bioavailability and antioxidant profile of ellagic acid by phospholipids. *J Agric Food Chem*. 2009;**57**(11):4559–65. doi: 10.1021/jf8037105. [PubMed: 19449806].

11. Pandey R, Ahmad Z, Sharma S, Khuller GK. Nano-encapsulation of azole antifungals: potential applications to improve oral drug delivery. *Int J Pharm*. 2005;**301**(1-2):268–76. doi: 10.1016/j.ijpharm.2005.05.027. [PubMed: 16023808].
12. Kakran M, Sahoo NG, Li L. Dissolution enhancement of quercetin through nanofabrication, complexation, and solid dispersion. *Colloids Surf B Biointerfaces*. 2011;**88**(1):121–30. doi: 10.1016/j.colsurfb.2011.06.020. [PubMed: 21764266].
13. Muller RH, Mader K, Gohla S. Solid lipid nanoparticles (SLN) for controlled drug delivery - a review of the state of the art. *Eur J Pharm Biopharm*. 2000;**50**(1):161–77. [PubMed: 10840199].
14. Mandawgade SD, Patravale VB. Development of SLNs from natural lipids: application to topical delivery of tretinoin. *Int J Pharm*. 2008;**363**(1-2):132–8. doi: 10.1016/j.ijpharm.2008.06.028. [PubMed: 18657601].
15. Garud A, Singh D, Garud N. Solid lipid nanoparticles (SLN): Method, characterization and applications. *Int Current Pharmaceutical J*. 2012;**1**(11):384–93.
16. Danhier F, Danhier P, De Saedeleer CJ, Fruytier AC, Schleich N, des Rieux A, et al. Paclitaxel-loaded micelles enhance transvascular permeability and retention of nanomedicines in tumors. *Int J Pharm*. 2015;**479**(2):399–407. doi: 10.1016/j.ijpharm.2015.01.009. [PubMed: 25578367].
17. Ngamcherdtrakul W, Morry J, Gu S, Castro DJ, Goodyear SM, Sangvanich T, et al. Cationic Polymer Modified Mesoporous Silica Nanoparticles for Targeted SiRNA Delivery to HER2+ Breast Cancer. *Adv Funct Mater*. 2015;**25**(18):2646–59. doi: 10.1002/adfm.201404629. [PubMed: 26097445].
18. Amiji MM. *Nanotechnology for cancer therapy*. CRC press; 2006.
19. Liu Y, Jie X, Guo Y, Zhang X, Wang J, Xue C. Green Synthesis of Oxovanadium(IV)/chitosan Nanocomposites and Its Ameliorative Effect on Hyperglycemia, Insulin Resistance, and Oxidative Stress. *Biol Trace Elem Res*. 2016;**169**(2):310–9. doi: 10.1007/s12011-015-0420-6. [PubMed: 26144273].
20. Kathe N, Henriksen B, Chauhan H. Physicochemical characterization techniques for solid lipid nanoparticles: principles and limitations. *Drug Dev Ind Pharm*. 2014;**40**(12):1565–75. doi: 10.3109/03639045.2014.909840. [PubMed: 24766553].
21. Li B, Harich K, Wegiel L, Taylor LS, Edgar KJ. Stability and solubility enhancement of ellagic acid in cellulose ester solid dispersions. *Carbohydr Polym*. 2013;**92**(2):1443–50. doi: 10.1016/j.carbpol.2012.10.051. [PubMed: 23399175].
22. Sonaje K, Italia JL, Sharma G, Bhardwaj V, Tikoo K, Kumar MN. Development of biodegradable nanoparticles for oral delivery of ellagic acid and evaluation of their antioxidant efficacy against cyclosporine A-induced nephrotoxicity in rats. *Pharm Res*. 2007;**24**(5):899–908. doi: 10.1007/s11095-006-9207-y. [PubMed: 17377747].
23. Ezzati Nazhad Dolatabadi J, Hamishehkar H, Eskandani M, Valizadeh H. Formulation, characterization and cytotoxicity studies of alendronate sodium-loaded solid lipid nanoparticles. *Colloids Surf B Biointerfaces*. 2014;**117**:21–8. doi: 10.1016/j.colsurfb.2014.01.055. [PubMed: 24607519].
24. Martins S, Costa-Lima S, Carneiro T, Cordeiro-da-Silva A, Souto EB, Ferreira DC. Solid lipid nanoparticles as intracellular drug transporters: an investigation of the uptake mechanism and pathway. *Int J Pharm*. 2012;**430**(1-2):216–27. doi: 10.1016/j.ijpharm.2012.03.032. [PubMed: 22465548].
25. Hamishehkar H, Shokri J, Fallahi S, Jahangiri A, Ghanbarzadeh S, Kouhsoltani M. Histopathological evaluation of caffeine-loaded solid lipid nanoparticles in efficient treatment of cellulite. *Drug Dev Ind Pharm*. 2015;**41**(10):1640–6. doi: 10.3109/03639045.2014.980426. [PubMed: 25382163].
26. Arulmozhi V, Pandian K, Mirunalini S. Ellagic acid encapsulated chitosan nanoparticles for drug delivery system in human oral cancer cell line (KB). *Colloids Surf B Biointerfaces*. 2013;**110**:313–20. doi: 10.1016/j.colsurfb.2013.03.039. [PubMed: 23732810].
27. Eskandani M, Nazemiyeh H. Self-reporter shikonin-Act-loaded solid lipid nanoparticle: formulation, physicochemical characterization and geno/cytotoxicity evaluation. *Eur J Pharm Sci*. 2014;**59**:49–57. doi: 10.1016/j.ejps.2014.04.009. [PubMed: 24768857].
28. Wang Y, Zhu L, Dong Z, Xie S, Chen X, Lu M, et al. Preparation and stability study of norfloxacin-loaded solid lipid nanoparticle suspensions. *Colloids Surf B Biointerfaces*. 2012;**98**:105–11. doi: 10.1016/j.colsurfb.2012.05.006. [PubMed: 22659379].
29. Aggarwal BB, Shishodia S. Molecular targets of dietary agents for prevention and therapy of cancer. *Biochem Pharmacol*. 2006;**71**(10):1397–421. doi: 10.1016/j.bcp.2006.02.009. [PubMed: 16563357].
30. Malik A, Afaq S, Shahid M, Akhtar K, Assiri A. Influence of ellagic acid on prostate cancer cell proliferation: a caspase-dependent pathway. *Asian Pac J Trop Med*. 2011;**4**(7):550–5. doi: 10.1016/S1995-7645(11)60144-2. [PubMed: 21803307].
31. Kirkin V, Joos S, Zornig M. The role of Bcl-2 family members in tumorigenesis. *Biochim Biophys Acta*. 2004;**1644**(2-3):229–49. doi: 10.1016/j.bbamcr.2003.08.009. [PubMed: 14996506].
32. Mbazima VG, Mokgotho MP, February F, Rees DJG, Mampuru L. Alteration of Bax-to-Bcl-2 ratio modulates the anticancer activity of methanolic extract of Commelina benghalensis (Commelinaceae) in Jurkat T cells. *African J Biotechnol*. 2008;**7**(20).